General and Comparative Endocrinology 277 (2019) 73–81

Contents lists available at ScienceDirect

General and Comparative Endocrinology

journal homepage: www.elsevier.com/locate/ygcen

Pharmacology of the giant panda (*Ailuropoda melanoleuca*) melanocortin-3 receptor

Hai-Jie Zhang[a,b], Hua-Jie Xie[a], Wei Wang[b,1], Zhi-Qiang Wang[a,*], Ya-Xiong Tao[b,*]

[a] Jiangsu Co-innovation Center for Prevention and Control of Important Animal Infectious Diseases and Zoonoses, College of Veterinary Medicine, Yangzhou University, Yangzhou, Jiangsu 225009, People's Republic of China

[b] Department of Anatomy, Physiology and Pharmacology, College of Veterinary Medicine, Auburn University, Auburn, AL 36849, United States

ARTICLE INFO

Keywords:
Melanocortin-3 receptor
Giant panda
Binding
Signaling
Western blot

ABSTRACT

The melanocortin-3 receptor (MC3R) is a member of the G protein-coupled receptor superfamily that plays a critical role in controlling energy balance and metabolism. Although pharmacological characterization of MC3R has been reported previously in several other species, there is no report on the MC3R from giant panda (*Ailuropoda melanoleuca*). This ancient species is known as a 'living fossil' and is among the most endangered animals in the world. Giant panda survive on a specialized diet of bamboo despite possessing a typical carnivorous digestive system. We report herein the molecular cloning and pharmacological characterization of amMC3R. Homology and phylogenetic analysis showed that amMC3R was highly homologous (> 85%) to several other mammalian MC3Rs. Using human MC3R (hMC3R) as a control, the binding of five agonists, [Nle^4, D-Phe^7]-α-melanocyte stimulating hormone (NDP-MSH), α-, β-, γ-, and D-Trp^8-γ-MSH, was investigated, as well as Gs-cAMP and pERK1/2 signaling. The results showed that amMC3R bound NDP- and D-Trp^8-γ-MSH with the highest affinity, followed by α-, β-, and γ-MSH, with the same rank order as hMC3R. When stimulated with agonists, amMC3R displayed increased intracellular cAMP and activation of pERK1/2. These data suggest that the cloned amMC3R was a functional receptor. The availability of amMC3R and knowledge of its pharmacological functions will assist further investigation of its role in controlling energy balance and metabolism.

1. Introduction

The melanocortin system consists of melanocortin peptides derived from tissue-specific post-translational processing of proopiomelanocortin (POMC), including adrenocorticotropic hormone (ACTH) and α-, β-, and γ-melanocyte-stimulating hormones (MSHs), and five known melanocortin receptor (MCR) subtypes (MC1R – MC5R) (Dores et al., 2014; Tao, 2017). MCRs have seven transmembrane domains and are typical members of Family A, rhodopsin-like G protein-coupled receptors (GPCRs). The MC1R, previously referred to as the MSH receptor, is expressed on melanocytes and melanophores, and plays a key role in regulating the synthesis of epidermal melanin pigments (Herraiz et al., 2017). The MC2R, also referred as the ACTH receptor, is located on mammalian adrenal cortex, and is an important component of the hypothalamus-pituitary-adrenal gland axis responding to stress. The MC5R is expressed in some exocrine glands and regulates synthesis and secretion of exocrine gland products (Cone, 2006).

The MC3R and MC4R play critical roles in the regulation of energy homeostasis. The MC4R is critical in regulating food intake and energy expenditure, and mice lacking *Mc4r* exhibit severe obesity due to increased food intake and decreased energy expenditure, as well as hyperinsulinemia (Huszar et al., 1997). The MC3R was first cloned from human and rat in 1993 (Gantz et al., 1993; Roselli-Rehfuss et al., 1993), and is expressed in multiple brain regions, and co-expressed with MC4R specifically in the arcuate nucleus and ventromedial nuclei of the hypothalamus and limbic system. It is also expressed in intestine and placenta but not in several other peripheral tissues such as heart, liver, lung, testes, and thyroid (Gantz et al., 1993; Roselli-Rehfuss et al., 1993). More recent data detected MC3R at both the mRNA and protein levels in mouse immune cells including macrophages (Getting et al., 2003).

Known endogenous agonists of MC3R include α-, β- and γ-MSHs, and Agouti-related protein (AgRP) is an endogenous antagonist (Ollmann et al., 1997). Upon agonist stimulation, MC3R couples to the stimulatory heterotrimeric G protein (Gs) and activates adenylyl cyclase to promote the intracellular accumulation of cAMP. *In situ*

* Corresponding authors.
E-mail addresses: zqwang@yzu.edu.cn (Z.-Q. Wang), taoyaxi@auburn.edu (Y.-X. Tao).
[1] Current address: Department of Clinical Laboratory, Xiamen Huli Guoyu Clinic, Co., Ltd., Xiamen, People's Republic of China.

https://doi.org/10.1016/j.ygcen.2018.10.024
Received 25 July 2018; Received in revised form 13 October 2018; Accepted 30 October 2018
Available online 01 November 2018
0016-6480/

A

```
1   ATG GAA CAA AAG CTG ATC TCA GAA GAA GAC CTA AAC GCT TCG TGC TGC CTG CTG CCT GCT  30
1   M   E   Q   K   L   I   S   E   E   D   L   N   A   S   C   C   L   L   P   A  10

31  CAG CCA ACA CTG CCG AAC AGC TCA GAG CAC CTC GCA GCC CCC TCC TTC AGC AAC CAG AGC  90
11  Q   P   T   L   P   N   S   S   E   H   L   A   A   P   S   F   S   N   Q   S  30

91  AGC AGC GGC TTC TGC GAG CAG GTC TTC ATC AAG CCC GAA GTC TTC CTG GCG CTG GGC ATC 150
31  S   S   G   F   C   E   Q   V   F   I   K   P   E   V   F   L   A   L   G   I  50

151 GTC AGC CTG ATG GAA AAC ATC CTG GTC ATC CTG GCC GTG GTC AGG AAC GGC AAC CTG CAC 210
51  V   S   L   M   E   N   I   L   V   I   L   A   V   V   R   N   G   N   L   H  70

211 TCC CCC ATG TAC TTC TTC CTC TGC AGC CTG GCC GTG GCC GAC ATG CTC GTG AGC GTG TCC 270
71  S   P   M   V   F   F   L   C   S   L   A   V   A   D   M   L   V   S   V   S  90

271 AAC GCC CTG GAG ACC ATC ATG ATC GCC ATC ATC AAC AGC AAC TAC CTG ACC TTC GAG GAC 330
91  N   A   L   E   T   I   M   I   A   I   I   N   S   N   Y   L   T   F   E   D 110

331 CAG TTC ATC CAG CAC ATG GAC AAC GTC TTC GAC TCC ATG ATC TGC ATC TCC CTG GTG GCC 390
111 Q   F   I   Q   H   M   D   N   V   F   D   S   M   I   C   I   S   L   V   A 130

391 TCC ATC TGC AAC CTC CTG GCC ATC GCC GTG GAC AGG TAC GTC ACC ATC TTC TAT GCG CTC 450
131 S   I   C   N   L   L   A   I   A   V   D   R   Y   V   T   I   F   Y   A   L 150

451 CTT TAC CAC AGC ATC ATG AGC GTG CGG AAG GCC CTC GCC TGG ATC GTG GCC ATC TGG GTG 510
151 R   Y   H   S   I   M   S   V   R   K   A   L   A   W   I   V   A   I   W   V 170

511 TGC TGC GGC GTG TGC GGC GTG GTG TTC ATC GTC TAC TCC GAG AGC AAG ATG GTC ATC GTG 570
171 C   C   G   V   C   G   V   V   F   I   V   Y   S   E   S   K   M   V   I   V 190

571 TGC CTC ATC ACC ATG TTC TTC GCC ATG CTG CTG CTC ATG GGC ACC CTC TAC GTG CAC ATG 630
191 C   L   I   T   M   F   F   A   M   L   L   L   M   G   T   L   Y   V   H   M 210

631 TTC CTC TTC GCC CGG CTG CAC GTC CAG CGC ATC GCG GCG CTG CCA CCG GCC GAC GGG GTG 690
211 F   L   F   A   R   L   H   V   Q   R   I   A   A   L   P   P   A   D   G   V 230

691 GCC CCG CCG CAG CAC TCG TGC ATG AAG GGG GCC GTC ACC ATC ACC ATC CTG CTG GGG GTA 750
231 A   P   P   Q   H   S   C   M   K   G   A   V   T   I   T   I   L   L   G   V 250

751 TTC ATC TTC TGC TGG GCC CCC TTC TTC CTC CAC CTC ATC CTC ATC ATA ACC TGC CCC ACC 810
251 F   I   F   C   W   A   P   F   F   L   H   L   I   L   I   I   T   C   P   T 270

811 AAC CCC TAC TGC GTC TGT TAC ACC GCC CAC TTC AAC ACC TAC CTC CTC CTT ATC ATG TGC 870
271 N   P   Y   C   V   C   Y   T   A   H   F   N   T   Y   L   V   L   I   M   C 290

871 AAC TCC GTC ATC GAC CCG CTC ATC TAC GCC TTC CGG AGC CTG GAG CTA CGC AAC ACG TTC 930
291 N   S   V   I   D   P   L   I   Y   A   F   R   S   L   E   L   R   N   T   F 310

931 AAG GAG ATC CTC TGC AGC TGC GAC GGC ATG AAC CTG GGG TAG
311 K   E   I   L   C   S   C   D   G   M   N   L   G   *
```

B

	Panda	Human	Mouse	Rat	Pig	Cattle	Sheep	Dog	Cat	Chicken	Zebrafish
Panda	100	91.3	87.8	89.4	91.4	91.6	92.4	96.2	92.2	74.5	68.2
Human		100	87.8	87.7	88.6	89.4	90.1	91.0	88.8	74.4	67.0
Mouse			100	93.0	85.6	86.4	87.1	87.8	86.6	74.7	67.8
Rat				100	86.4	87.2	87.3	89.1	87.4	74.6	68.2
Pig					100	89.7	91.0	91.6	89.0	72.5	68.5
Cattle						100	97.5	90.7	87.6	74.4	68.8
Sheep							100	92.0	89.1	74.2	68.4
Dog								100	92.5	73.8	68.1
Cat									100	71.9	68.6
Chicken										100	65.5
Zebrafish											100

C

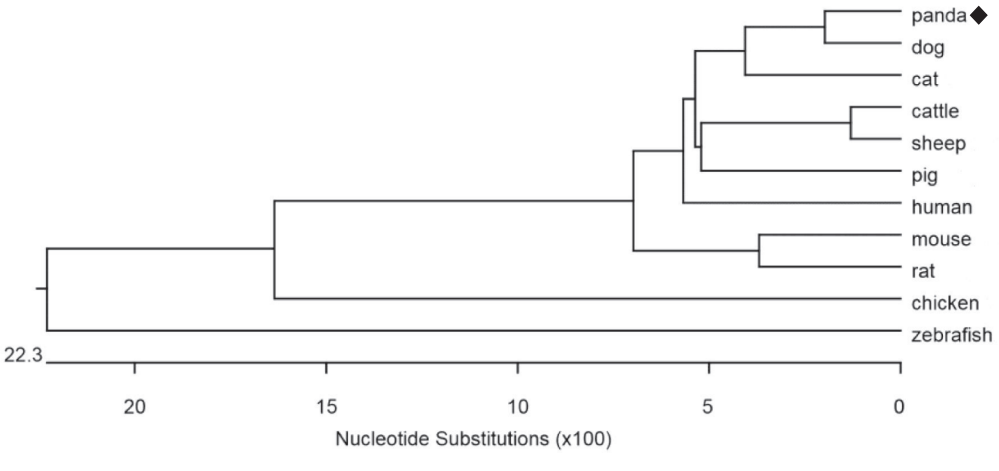

(caption on next page)

Fig. 1. Nucleotide and deduced amino acid sequences of the giant panda (*Ailuropoda melanoleuca*) MC3R (amMC3R) and comparison with MC3Rs from other species. (A) Sequence of the full-length amMC3R cDNA and *in silico* translation. The sequence of the myc tag is underlined. The seven transmembrane domains are shaded in grey. The highly conserved DRY and N/DPxxY motif (DPLIY in MC3R) are highlighted in italics. (B) Homology and (C) phylogenetic analysis of MC3R nucleotide sequences from several species.

hybridization studies indicated that like *POMC* mRNA, *MC3R* mRNA is also expressed in the arcuate nucleus, suggesting that MC3R can also act as an inhibitory auto-receptor in POMC neurons (Marks et al., 2006). However, unlike MC4R, when treated with D-Trp^8-γ-MSH, MC3R dampens POMC neuronal activity (Marks et al., 2006). A previous study showed that *Mc3r* knockout mice do not exhibit increased food intake or weight gain (Chen et al., 2000), but although the total body weight remains the same, the ratio of fat is increased by ~40% compared with wild-type mice (Butler et al., 2000). Although *Mc3r* knockout mice display an increase in adiposity, these animals are protected against the development of metabolic syndrome compared with other mouse models with comparable levels of adiposity (Trevaskis et al., 2007). In humans, despite earlier failures in identifying clinically relevant mutations in the *MC3R* (see (Hani et al., 2001; Li et al., 2000) for examples), a series of subsequent investigations have identified mutations and polymorphisms in the *MC3R* that are associated with obesity, especially increased adiposity (Calton et al., 2009; Feng et al., 2005; Lee et al., 2007; Lee et al., 2002; Rached et al., 2004; Savastano et al., 2009; Tao, 2007; Tao and Segaloff, 2004; Yang et al., 2015; Yang and Tao, 2012) (see (Demidowich et al., 2017; Tao, 2005, 2010; Yang and Tao, 2016b) for reviews). These studies highlight the importance of the MC3R in regulating energy balance in humans.

The giant panda (*Ailuropoda melanoleuca*), an ancient species known as a 'living fossil' with a history of ~7 million years, is one of the most endangered animals in China (Tang et al., 2008). This species survives on a specialized diet of bamboo, even though it has retained a typical carnivorous digestive system (Xue et al., 2015). This highly specialized feeding habit contributes to its endangered status, with less than 3000 giant pandas remaining in the wild (Zhan et al., 2006).

Since the melanocortin system is believed to play a significant role in the regulation of energy balance in mammals and other animals, we hypothesized that it may also be important for energy homeostasis in giant panda. We previously reported pharmacological studies on giant panda MC4R, demonstrating that panda MC4R and human MC4R share the same rank order for the binding of several melanocortin peptides (Wang et al., 2016). However, there is no report on giant panda MC3R yet. To investigate the role of MC3R in regulating energy homeostasis and other physiological functions in giant panda, we report herein the molecular cloning and pharmacological characterization of the giant panda MC3R (amMC3R). We analyzed the sequence characteristics of the protein encoded by the am*MC3R* gene and compared it with homologs from human and other species. Using the human MC3R (hMC3R) as a control, the ligand binding and signaling properties of amMC3R were investigated using several MC3R agonists, including [Nle^4, D-Phe^7]-α-MSH (NDP-MSH), and α-, β-, γ-, and D-Trp^8-γ-MSH.

Although the MC3R pharmacology have been studied in several species, the panda MC3R pharmacology was still unknown. Previous studies have highlighted important differences in orthologs of the same GPCR from different species. For example, dramatic differences in wild-type or mutation-induced constitutive activities have been observed in cholecystokinin-B/gastrin receptor (Schaffer et al., 1998), follitropin receptor (Tao et al., 2002), MC3R (Renquist et al., 2012), and MC4R (Li et al., 2016; Li et al., 2017; Yi et al., 2018). Drug efficacy and potency can also be different between species homologs (Jiang et al., 2008; Kopin et al., 1997; Ndong et al., 2011), important considerations when using different animal models and potential applications in animal production. Porcine somatostatin receptor 2 has been shown to have different pharmacological properties compared with the human homolog (Durán-Prado et al., 2007). Significant difference in receptor pharmacology has even been observed in homologs from very closely related species such as cynomolgus monkey and human (Hipkin et al., 2004). Therefore the present study on panda MC3R pharmacology was relevant.

2. Materials and methods

2.1. Hormones and supplies

NDP-MSH and D-Trp^8-γ-MSH were purchased from Peptides International (Louisville, KY, USA). α-MSH and γ-MSH were purchased from Pi Proteomics (Huntsville, AL, USA). β-MSH was purchased from CHI Scientific (Maynard, MA, USA). ^{125}I-NDP-MSH was iodinated as previously described (Mo et al., 2012). ^{125}I-cAMP was iodinated using the chloramine T method (Tao et al., 2010). Tissue culture plasticware was purchased from Corning (Corning, NY, USA). Cell culture media, newborn calf serum, and other reagents for cell culture were obtained from Invitrogen (Carlsbad, CA, USA). Human MC3R expression vector was described in our previous article (Tao and Segaloff, 2004).

2.2. Molecular cloning of amMC3R

The sequence of am*MC3R* in the NCBI database indicated a putative coding region with a single exon of 972 bp. The coding DNA sequence was amplified directly from giant panda genomic DNA using sense primer 5′-CCGGAATTCATGAACGCTTCGCGCTGCCTGCTGCC-3′ and antisense primer 5′-CCTCTAGACTACCCCAGGTTAATGCCGTCGCAG CTG-3′ based on the published nucleotide sequence of amMC3R (NCBI reference sequence number XM_002921212.2), incorporating *Eco*RI and *Xba*I restriction sites in sense and antisense primers (underlined), respectively. PCR amplification was performed in a 25 µl mixture containing 100 ng of giant panda genomic DNA (Wang et al., 2016), 0.4 µM of each primer, and 12.5 µl 2 × Easy Taq PCR SuperMix (Trans-Gen Biotech, Nanjing, China), with the following cycling parameters: 5 min at 94 °C for one cycle, followed by 60 s at 94 °C, 60 s at 56 °C, and 90 s at 72 °C for 35 cycles, then a final extension at 72 °C for 10 min. After amplification, PCR products were separated by electrophoresis on a 1.5% agarose gel with 1 × TAE buffer, stained with ethidium bromide, and visualized under UV light. PCR products of the expected size were excised and purified from the gel using an Axygen PCR purification kit (Axygen, Beijing, China), double digested with *Eco*RI and *Xba*I (Promega, Shanghai, China), and ligated into the expression vector pcDNA3.1(+) using T4 DNA ligase (Trans-Gen Biotech) at 16 °C overnight.

Recombinant plasmids were transformed into competent *Escherichia coli* DH5α cells and spread on an LB-agar plate containing 50 µg/ml ampicillin. Plasmid DNA was extracted from cultures grown from single colonies using an Axygen mini-preparation kit, and clones were screened for an insert of the expected size by digestion with *Eco*RI and *Xba*I. The nucleotide sequence of the cloned amMC3R was determined for three independent plasmids at Sangon Biotech Co. Ltd (Shanghai, China). After verifying that the entire coding region was intact by automated DNA sequencing, amMC3R tagged at its N-terminus (after the initiating Met codon) with a myc tag was generated by Sangon Biotech. The addition of a myc epitope tag facilitates future experiments such as immunofluorescence or immunoblotting when an antibody is needed because the antibodies for GPCRs are mostly of poor quality and the antibodies for myc epitope tag have been validated in numerous publications. Extensive studies including our own on the MC4R have shown that small epitope tags like myc do not affect receptor pharmacology (Tao and Segaloff, 2003). Plasmid DNA containing a myc epitope tag

A

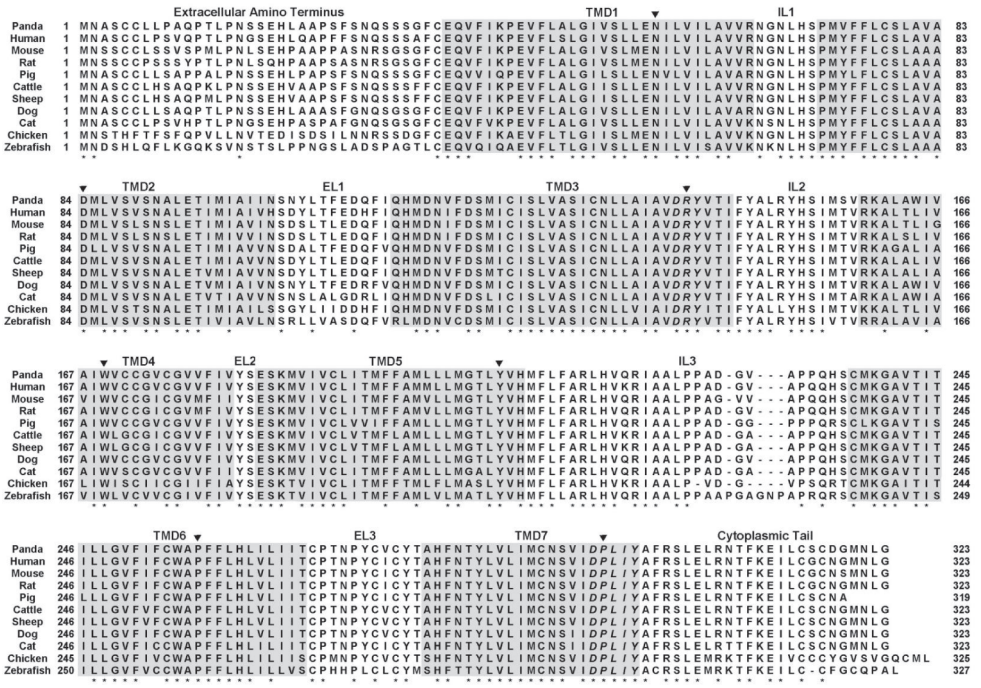

B

	Panda	Human	Mouse	Rat	Pig	Cattle	Sheep	Dog	Cat	Chicken	Zebrafish
Panda	100	92.9	87.3	89.2	89.3	92.9	92.0	95.7	88.5	76.3	72.4
Human		100	88.9	89.8	87.5	92.0	91.0	92.3	86.7	76.0	70.2
Mouse			100	94.7	83.1	87.3	87.0	86.7	84.8	74.1	69.6
Rat				100	84.3	88.9	87.9	88.5	85.1	74.8	70.8
Pig					100	88.7	88.4	89.3	83.1	71.6	71.7
Cattle						100	98.8	92.3	86.7	76.3	72.4
Sheep							100	92.0	87.0	75.4	71.7
Dog								100	89.8	75.4	71.4
Cat									100	72.9	71.4
Chicken										100	79.8
Zebrafish											100

C

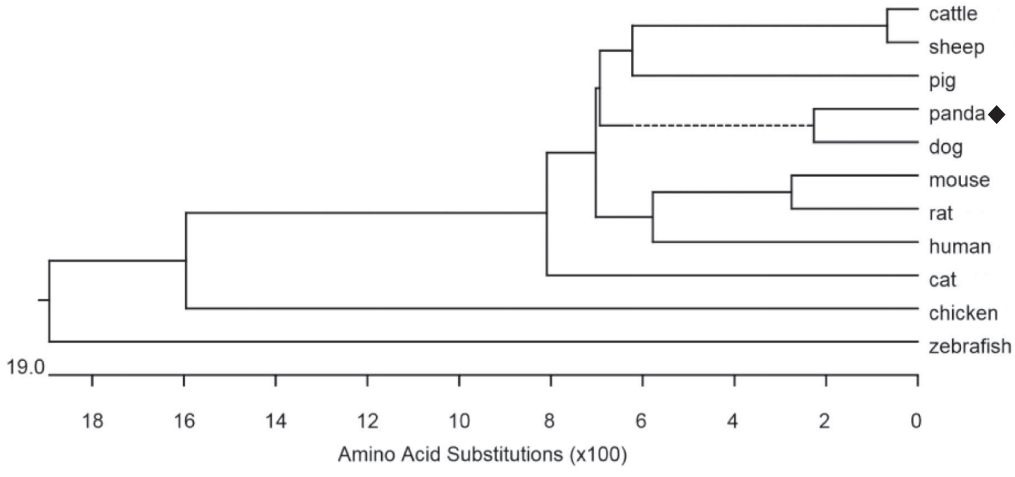

(caption on next page)

Fig. 2. Comparison of the amino acid sequence of amMC3R with those of MC3Rs from other species. The amMC3R sequence is aligned with those of human (hMC3R), mouse (mMC3R), rat (rMC3R), pig (pMC3R), cattle (cMC3R), sheep (sMC3R), dog (dMC3R), cat (cMC3R), chicken (gMC3R), and zebrafish (zMC3R). Positions of different regions are indicated above the sequences and labelled as follows: transmembrane domain, TMD; extracellular loop, EL; intracellular loop, IL; amino and carboxyl termini, extracellular amino terminus and intracellular cytoplasmic tail, respectively. Conserved residues are indicated with an asterisk (*). The transmembrane domains are shaded grey, with the most conserved residue in each transmembrane domain indicated by an inverted filled triangle. (B) Homology and (C) phylogenetic analysis of MC3R amino acid sequences from several species.

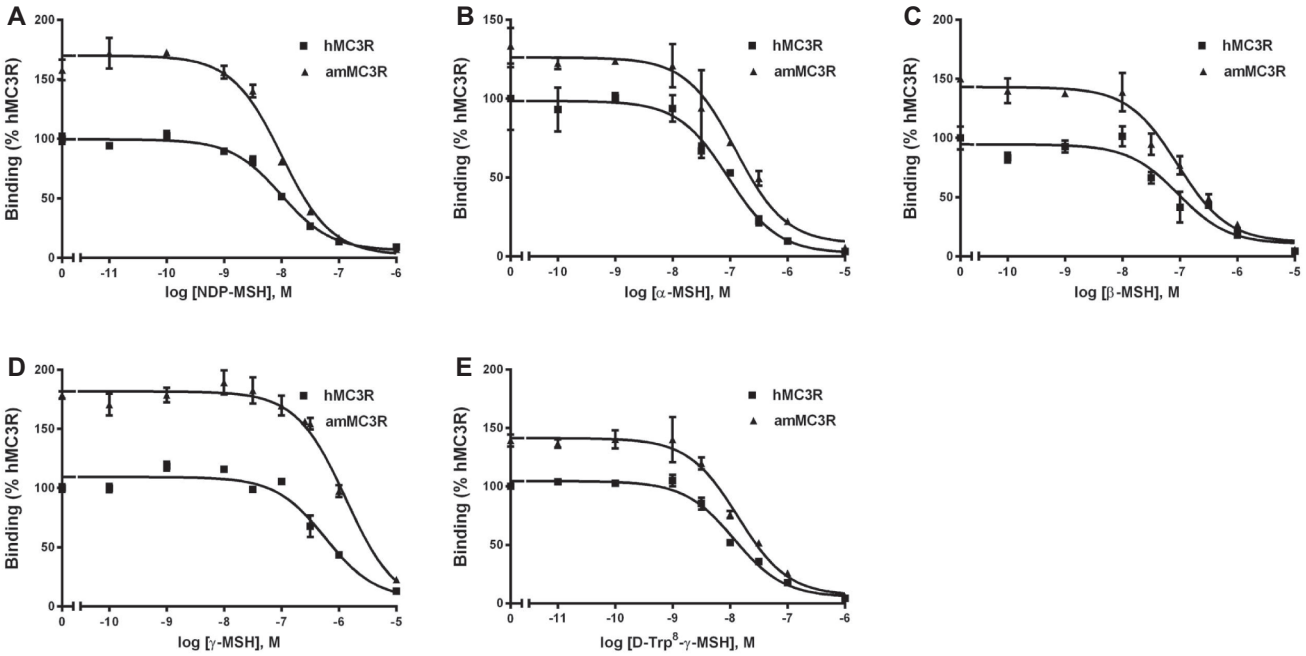

Fig. 3. Ligand binding properties of the cloned amMC3R in HEK293T cells. HEK293T cells were transiently transfected with the cloned amMC3R (hMC3R was used as a control), and binding properties of the MC3Rs were measured as described in Section 2. Different concentrations of unlabeled agonists were used to displace the binding of ^{125}I-NDP-MSH to MC3Rs in intact cells (A, NDP-MSH; B, α-MSH; C, β-MSH; D, γ-MSH; E, D-Trp^8-γ-MSH). Results are expressed as mean % of hMC3R binding ± range from duplicate determinations within one experiment. All experiments were performed three times.

Table 1
Ligand binding properties of amMC3R.

	n	B_{max} (%)	IC_{50} (nM)				
			NDP-MSH	α-MSH	β-MSH	γ-MSH	D-Trp^8-γ-MSH
hMC3R	3	100	9.26 ± 1.12	95.85 ± 1.89	90.27 ± 3.51	609.47 ± 18.47	19.61 ± 4.21
amMC3R	3	148 ± 6.56	8.33 ± 1.55	123.48 ± 17.54*	104.06 ± 7.54*	1755.3 ± 265.9*	29.08 ± 8.02

Abbreviations: Bmax, binding capacity; IC_{50}, concentration of unlabeled ligand resulted in 50% displacement.
Values are expressed as the mean ± S.E.M. of at least three independent experiments.
* Significant differences from the hMC3R control, $p < 0.05$.

and the correct amMC3R sequence (myc-amMC3R-pcDNA3.1) was prepared with an Axygen Plasmid Maxi kit for transfection as described below.

2.3. Homology and phylogenetic analysis of amMC3R

Homology and phylogenetic analyses at nucleotide and amino acid levels were performed for sequences from various species including giant panda (*A. melanoleuca*), human (*Homo sapiens*), mouse (*Mus musculus*), rat (*Rattus norvegicus*), cattle (*Bos taurus*), pig (*Sus scrofa*), sheep (*Ovis aries*), dog (*Canis lupus*), cat (*Felis catus*), chicken (*Gallus gallus*), and zebrafish (*Danio rerio*) using the DNASTAR 7.0.0 program according to the manufacturer's protocol (Madison, WI, USA).

2.4. Cells and transfections

Human embryonic kidney (HEK) 293T cells, purchased from American Type Culture Collection (Manassas, VA, USA), were grown at 5% CO_2 in Dulbecco's Modified Eagle's Medium (DMEM) supplemented with 50 μg/ml of gentamicin, 100 IU/ml of penicillin, 100 μg/ml of streptomycin, 20 μg/ml of amphotericin B, 10 mM HEPES, and 10% newborn calf serum. Cells were plated on gelatin-coated 35 mm six-well clusters from Corning. For transient expression of myc-amMC3R, when cells reached 50–70% confluency, plasmids were transfected using the calcium phosphate precipitation method (Chen and Okayama, 1987). At ~48 h after transient transfection, measurement of ligand binding and ligand-stimulated cAMP generation and phosphorylated ERK1/2 were performed.

2.5. Radioligand binding assay

Ligand binding assays were performed as described previously (Tao and Segaloff, 2003). Briefly, at 48 h after transient transfection, HEK293T cells were washed twice with pre-warmed Waymouth's media (Sigma-Aldrich, St. Louis, MO, USA) containing 1 mg/ml bovine serum albumin (BSA; referred herein as Waymouth/BSA). Fresh Waymouth/

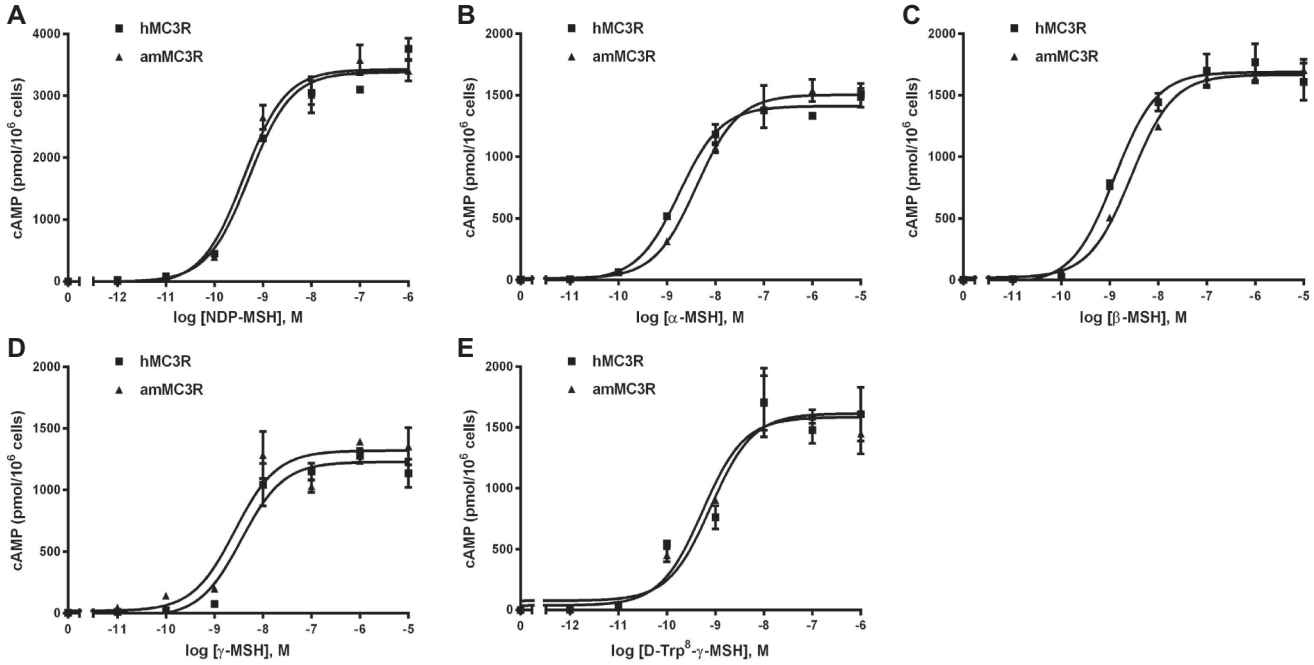

Fig. 4. Signaling properties of the cloned amMC3R in HEK293T cells. HEK293T cells were transiently transfected with the cloned amMC3R (hMC3R was used as a control), and signaling assays were performed as described in Section 2. For measurement of cAMP accumulation, transfected cells were stimulated with various concentrations of agonists (A, NDP-MSH; B, α-MSH; C, β-MSH; D, γ-MSH; E, D-Trp^8-γ-MSH). Intracellular cAMP levels were measured by radioimmunoassay. Results are expressed as the mean ± S.E.M. of triplicate determinations within one experiment, and all experiments were performed three times.

Table 2
Agonist-stimulated cAMP responses of hMC3R and amMC3R.

	n	NDP-MSH		α-MSH		β-MSH		γ-MSH		D-Trp^8-γ-MSH	
		EC_{50} (nM)	R_{max}	EC_{50} (nM)	R_{max}	EC_{50} (nM)	R_{max}	EC_{50} (nM)	R_{max}	EC_{50} (nM)	R_{max}
hMC3R	3	0.58 ± 0.12	100	3.68 ± 1.00	100	2.10 ± 0.43	100	2.80 ± 0.44	100	0.46 ± 0.18	100
amMC3R	3	0.63 ± 0.12	109 ± 4	4.99 ± 2.17	116 ± 10	4.71 ± 1.48	102 ± 4	5.06 ± 1.29*	97 ± 6	0.57 ± 0.10*	98 ± 2

Abbreviations: $EC_{50,}$ concentration of agonist causing 50% stimulation of the maximal response; $R_{max,}$ maximal response.
Data are expressed as the mean ± S.E.M. of three independent experiments. The R_{max} was 3238 ± 276 pmol/10^6 cells for hMC3R under NDP-MSH stimulation, 1565 ± 104 pmol/10^6 cells under α-MSH stimulation, 1735 ± 29 pmol under β-MSH stimulation, 1648 ± 222 pmol under γ-MSH stimulation, and 1595 ± 174 pmol/10^6 cells under D-Trp^8-γ-MSH stimulation.

BSA with or without different concentrations of unlabeled ligands (NDP-, α-, β-, γ- or D-Trp^8-γ-MSH) containing 100,000 cpm of ^{125}I-NDP-MSH was then incubated at 37 °C for 1 h. The total volume was 1 ml in each well, and the final concentrations of unlabeled ligands are indicated in the figures. After incubation, plates were placed directly on ice and washed twice with cold Hanks' balanced salt solution containing 1 mg/ml BSA to terminate the reaction. Cells were then solubilized with 100 µl of 0.5 M NaOH, and cell lysates were collected with cotton swabs and counted in a gamma counter. All determinations were performed in duplicate, and the experiment was repeated at least three times. B_{max} (maximal binding) and IC_{50} (the concentration of unlabeled ligand resulting in 50% displacement) were calculated using GraphPad Prism 4.0 software (San Diego, CA, USA).

2.6. Ligand-stimulated cAMP generation

Transient transfection of HEK293T cells was performed as described above. At about 48 h after transient transfection, HEK293T cells were washed twice with warm Waymouth/BSA, and fresh Waymouth/BSA containing 0.5 mM isobutylmethylxanthine (Sigma-Aldrich) was added to each well and incubated at 37 °C for 15 min. Next, either buffer alone or different concentrations of ligands (NDP-, α-, β-, γ- or D-Trp^8-γ-MSH) were added to each well, with the final volume adjusted to 1 ml, and cells were incubated at 37 °C for another 1 h. The final ligand concentrations are indicated in the figures. After incubation, cells were placed on ice to terminate the reaction, media were aspirated, and intracellular cAMP was extracted with 0.5 M perchloric acid containing 180 mg/ml theophylline. The cAMP concentration was measured by radioimmunoassay (Tao et al., 2010). All determinations were performed in triplicate, and the experiment was repeated at least three times. R_{max} (maximal response) and EC_{50} (the concentration of agonist causing 50% maximal cAMP production) were calculated using Prism 4.0 software.

2.7. Western blotting analysis

At 18 h after transient transfection, cells in 100-mm dish were washed twice and starved with Waymouth/BSA without serum. At 24 h after starvation, 4.5 ml of fresh Waymouth/BSA and 500 µl of the different ligands were added to each dish and cells were incubated at 37 °C for 5 min before cellular extraction. Cellular extracts were separated by 10% sodium dodecyl sulfate-polyacrylamide gel electrophoresis (SDS-PAGE) and transferred onto a PVDF membrane for immunoblotting. Specific rabbit primary antibodies were used for detection of phosphorylated forms of ERK1/2 (Thr^{202}/Tyr^{204}; 1:2500, Cell Signaling Technology, Danvers, MA, USA). Equal protein loading was verified by mouse β-tubulin antibody (1:2500, Developmental Studies Hybridoma Bank at the University of Iowa, IA, USA). Blots were probed with

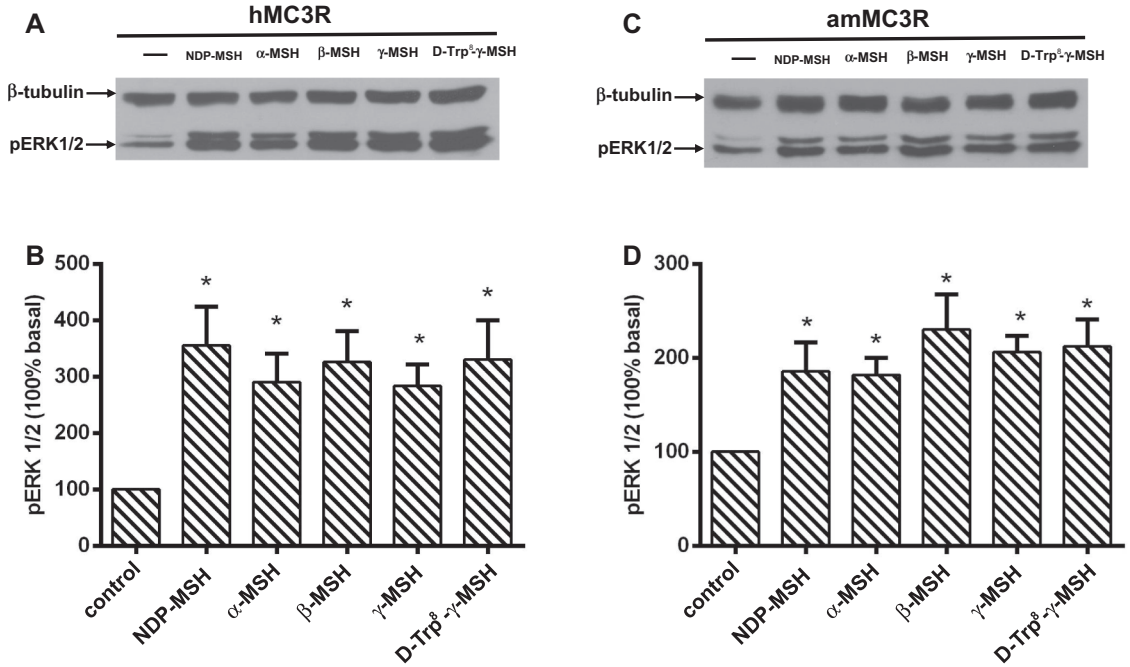

Fig. 5. ERK1/2 signaling of the cloned amMC3R in HEK293T cells. HEK293T cells were transiently transfected with the cloned amMC3R (hMC3R was used as a control), and western blots were performed as described in Section 2. For measurement of the activation of pERK1/2, transfected cells were stimulated with various agonists at different concentrations (NDP-MSH and D-Trp^8-γ-MSH at 10^{-6}M; α-MSH, β-MSH and γ-MSH at 10^{-5}M). Results are expressed as the mean ± S.E.M. of four independent experiments. Asterisks (*) indicate significant differences from basal pERK1/2 levels ($p < 0.05$).

horseradish peroxidase-conjugated anti-rabbit (1:2500) and anti-mouse (1:2500, Jackson ImmunoResearch Inc., West Grove, PA, USA) antibodies at room temperature for 1 h. Bound antibodies were detected using ECL reagent (Thermo Scientific, Waltham, IL, USA) and quantified by ImageJ 1.49 software (NIH, MD, USA).

2.8. Statistical analysis

GraphPad Prism 4.0 Software was used to calculate ligand binding, signaling, and pERK1/2 activation parameters including IC_{50}, EC_{50}, B_{max}, and R_{max}. Significance of differences in binding, signaling, and pERK1/2 activation parameters between human and giant panda WT MC3Rs were analyzed using Student's t-tests with Prism 4.0.

3. Results

3.1. Nucleotide and deduced amino acid sequences of putative amMC3R

The putative am*MC3R* gene published in the NCBI database (100469853) is intronless and contains one reading frame of 972 bp encoding a polypeptide of 323 amino acids (Fig. 1A). We designed forward and reverse primers to amplify the full-length am*MC3R* coding sequence, and the cloned sequence matched the predicted sequence perfectly. We performed nucleotide sequence alignment of the obtained nucleotide sequence of the am*MC3R* gene with nucleotide sequences of human, mouse, rat, pig, cattle, sheep, dog, cat, chicken, and zebrafish *MC3Rs* (GenBank accession number or NCBI reference sequence number NM_019888.3, NM_008561.3, NM_001025270.3, JQ828976.1, XM_002692426.1, XP_004014499.1, NP_001128596.1, XM_019826334.1, AB017137.1, and NP_851303.2, respectively). The comparison showed that giant panda *MC3R* shared 91.3%, 87.8%, 89.4%, 91.4%, 91.6%, 92.4%, 96.2%, 92.2%, 74.5%, and 68.2% homology with these other species at the nucleotide level (Fig. 1B). At the amino acid level, homology between giant panda MC3R was over 95.5% for dog, 92.0% for human, cattle, and sheep, 87.3–89.3% for mouse, rat, pig, and cat, 76.3% for chicken, and 72.4% for zebrafish (Fig. 2B). Like other GPCRs, amMC3R had seven transmembrane domains that are the most highly conserved regions among the different species.

3.2. Ligand binding properties of amMC3R with five MC3R ligands

In order to investigate the binding properties of amMC3R, competitive binding assays were preformed using whole-cell binding assays in HEK293T cells, using hMC3R for comparison. Different concentrations of five unlabeled ligands were used as competitors with a fixed amount of ^{125}I-NDP-MSH. NDP-MSH, a highly potent analog of the natural agonist (α-MSH), and D-Trp^8-γ-MSH, a selective analog of the natural agonist γ-MSH of MC3R, are widely used in MC3R studies. The endogenous ligands α-, β- and γ-MSHs were also used. As shown in Fig. 3, the maximal binding of the amMC3R was 148 ± 6.56% that of hMC3R, and the difference was statistically significant ($p < 0.05$). The amMC3R protein yielded significantly higher IC_{50} values compared to hMC3R for α-, β-, γ-, and D-Trp^8-γ-MSH ligands. However, when NDP-MSH was used, the two MC3Rs shared similar IC_{50} values (Table 1).

3.3. Signaling properties of amMC3R with five MC3R ligands

To further investigate whether the cloned *amMC3R* could respond to ligand stimulation to increase cAMP generation, radioimmunoassay was performed. We transiently transfected the amMC3R construct into HEK293T cells and analyzed the signaling properties using five MC3R ligands at different concentrations. As shown in Fig. 4, amMC3R caused a dose-dependent increase in intracellular cAMP when stimulated with all five agonists. Although the ligand binding assays revealed that the cloned amMC3R had relatively higher affinity compared with hMC3R, both receptors shared similar maximal responses when treated with NDP-, α-, β-, γ-, and D-Trp^8-γ-MSH and the EC_{50} values of the five ligands with amMC3R were comparable with those of hMC3R (Table 2). NDP-MSH and D-Trp^8-γ-MSH were more potent agonists at stimulating cAMP generation than the other agonists. Furthermore, the basal activity of amMC3R was similar to that of hMC3R.

3.4. pERK1/2 signaling efficacies of five MC3R agonists

To further evaluate the signaling properties of amMC3R, we measured the efficacy of several agonists in MAPK signaling. Previous studies found that activation of ERK1/2 induced by NDP-MSH is increased significantly at 5 min after stimulation with 1 μM NDP-MSH (Mo et al., 2012). We therefore chose 5 min as the stimulation duration, and used 10^{-6} M as the final concentration for both NDP-MSH and D-Trp^8-γ-MSH, since both are potent agonists of MC3Rs, whereas 10^{-5} M was used for the other agonists (α-, β-, and γ-MSH). As shown in Fig. 5, with amMC3R, all five agonists induced phosphorylation of ERK1/2, by ~2-fold. However, at the same concentration, phosphorylation of pERK1/2 was increased ~3-fold with hMC3R, and both receptors yielded comparable responses to all five agonists. The basal activity of amMC3R was similar to that of hMC3R.

4. Discussion

By bioinformatic analyses of giant panda genome, we identified the putative full-length coding region of am*MC3R*. Homology and phylogenetic analyses showed that among MC3Rs in different species, amMC3R was the most similar to the dog sequence, while unsurprisingly, the zebrafish sequence was the least similar to amMC3R, followed by chicken. The amino acid sequences of mammalian MC3Rs shared high conservation, including length and presumably structure, except for the pig MC3R (Fan et al., 2008), which is four amino acids shorter than other mammalian sequences. Previous studies showed that pig MC3R binds NDP-MSH with the highest affinity, followed by D-Trp^8-γ-MSH, γ-, and α-MSH, with the same ranking order as observed for hMC3R, although the affinity of pig MC3R for these ligands is between two- and nine-fold higher than that of hMC3R (Fan et al., 2008).

To further investigate the pharmacological function and physiological role in energy homeostasis of giant panda MC3R, ligand binding was performed using hMC3R for comparison. We wanted to find out whether amMC3R had similar affinity as hMC3R for the ligands. The experiments showed that amMC3R bound these ligands with the same rank order as the hMC3R, with the highest affinity for NDP-MSH, followed by D-Trp^8-γ-, α-, β-MSH, and γ-MSH. Comparison between the two receptors revealed that the affinities for all of the five ligands for hMC3R was higher than those for amMC3R. Our results showed that the IC_{50} values for these ligands were of the same order of magnitude as values determined in previous studies (Fan et al., 2008; Wang et al., 2008; Yang and Tao, 2012). Although amMC3R exhibited a comparatively high IC_{50} value, it displayed higher B_{max} compared with hMC3R.

MC3Rs regulate energy homoeostasis by receiving stimulation from certain POMC-derived peptides. As a member of the GPCR superfamily, the conventional signaling pathway of MC3R involves stimulation of adenylyl cyclase activity and consequent protein kinase A activation by coupling to Gs (Gantz et al., 1993; Roselli-Rehfuss et al., 1993). In the present study, we performed transient transfection of amMC3R in HEK293T cells. NDP-MSH and D-Trp^8-γ-MSH are long-lasting analogs of natural agonists α-MSH and γ-MSH, respectively, and the results revealed that the two analogs were more potent than the endogenous ligands. Among the five subtypes of MCRs, MC3R is the only one with high affinity for γ-MSH at physiological concentrations, and γ-MSH is widely considered as the probable endogenous ligand for this receptor (Humphreys et al., 2011). In our signaling experiments, when treated with β-MSH, the EC_{50} value was almost the same as α-MSH and γ-MSH, suggesting that β-MSH might also be an endogenous ligand of MC3R, and may play an important role in energy homoeostasis. Although the B_{max} value of amMC3R was higher than that of hMC3R, the R_{max} of the two receptors was comparable (Li et al., 2016), likely due to the presence of spare receptor in the transient transfection system (Tao, 2015).

In addition to the classical Gs-cAMP signaling pathway, other pathways could be activated by MC3R stimulation, including the MAPK pathway. HEK293T cells transiently transfected with MC3R can activate extracellular signal-regulated kinases 1 and 2 (ERK1/2) phosphorylation when treated with NDP-MSH (Chai et al., 2007), and cAMP production and ERK1/2 activation are not necessarily related (Yang and Tao, 2016a). Thus, to learn more about amMC3R, we further assessed the effects of the five ligands on ERK1/2, and all five agonists could induce ERK1/2 activation. Based on these and previously reported results, we used 10^{-6} M NDP-MSH and D-Trp^8-γ-MSH, and 10^{-5} M α-, β-, and γ-MSH as the final concentration for stimulating cells. The results showed that activation of ERK1/2 with amMC3R increased ~two-fold upon stimulation by agonists, while the increase with hMC3R was ~three-fold.

Previous studies showed that MC3R is expressed in several other tissues in addition to the brain, including gastrointestinal tract, pituitary gland, placenta, immune cells and but not in several other peripheral tissues such as heart, liver, lung, testes, and thyroid (Gantz et al., 1993; Getting et al., 1999; Regard et al., 2008; Roselli-Rehfuss et al., 1993). However, because of the endangered status of the giant panda, we cannot obtain tissues from giant panda. Therefore we cannot study tissue expression of amMC3R. This is a limitation of the current study.

In conclusion, giant panda MC3R was successfully cloned and inserted into the eukaryotic expression vector pcDNA3.1. The recombinant plasmid was transiently transfected into HEK293T cells, and pharmacological experiments revealed that amMC3R exhibited full functionality upon stimulation with agonists *in vitro*. Compared with hMC3R, the two receptors shared the same rank order for the binding of five tested agonists, and yielded similar signaling results in two pathways. These findings lay the foundation for further study of the role of amMC3R in giant panda physiology.

Acknowledgements

This work was supported by the National Natural Science Foundation of China (grant number 31872526 and 31572571), Priority Academic Program Development of Jiangsu Higher Education Institutions, and Animal Health and Disease Research Program of Auburn University College of Veterinary Medicine. Wei Wang was supported by a fellowship from China Scholarship Council, People's Republic of China.

Appendix A. Supplementary data

Supplementary data to this article can be found online at https://doi.org/10.1016/j.ygcen.2018.10.024.

References

Butler, A.A., Kesterson, R.A., Khong, K., Cullen, M.J., Pelleymounter, M.A., Dekoning, J., Baetscher, M., Cone, R.D., 2000. A unique metabolic syndrome causes obesity in the melanocortin-3 receptor-deficient mouse. Endocrinology 141, 3518–3521.

Calton, M.A., Ersoy, B.A., Zhang, S., Kane, J.P., Malloy, M.J., Pullinger, C.R., Bromberg, Y., Pennacchio, L.A., Dent, R., McPherson, R., Ahituv, N., Vaisse, C., 2009. Association of functionally significant Melanocortin-4 but not Melanocortin-3 receptor mutations with severe adult obesity in a large North American case-control study. Hum. Mol. Genet. 18, 1140–1147.

Chai, B., Li, J.Y., Zhang, W., Ammori, J.B., Mulholland, M.W., 2007. Melanocortin-3 receptor activates MAP kinase via PI3 kinase. Regul. Pept. 139, 115–121.

Chen, A.S., Marsh, D.J., Trumbauer, M.E., Frazier, E.G., Guan, X.M., Yu, H., Rosenblum, C.I., Vongs, A., Feng, Y., Cao, L., Metzger, J.M., Strack, A.M., Camacho, R.E., Mellin, T.N., Nunes, C.N., Min, W., Fisher, J., Gopal-Truter, S., MacIntyre, D.E., Chen, H.Y., Van der Ploeg, L.H., 2000. Inactivation of the mouse melanocortin-3 receptor results in increased fat mass and reduced lean body mass. Nat. Genet. 26, 97–102.

Chen, C., Okayama, H., 1987. High-efficiency transformation of mammalian cells by plasmid DNA. Mol. Cell. Biol. 7, 2745–2752.

Cone, R.D., 2006. Studies on the physiological functions of the melanocortin system. Endocr. Rev. 27, 736–749.

Demidowich, A.P., Jun, J.Y., Yanovski, J.A., 2017. Polymorphisms and mutations in the melanocortin-3 receptor and their relation to human obesity. BBA 1863, 2468–2476.

Dores, R.M., Londraville, R.L., Prokop, J., Davis, P., Dewey, N., Lesinski, N., 2014. Molecular evolution of GPCRs: melanocortin/melanocortin receptors. J. Mol. Endocrinol. 52, T29–T42.

Durán-Prado, M., Bucharles, C., Gonzalez, B.J., Vázquez-Martínez, R., Martínez-Fuentes, A.J., García-Navarro, S., Rhodes, S.J., Vaudry, H., Malagón, M.M., Castaño, J.P., 2007. Porcine somatostatin receptor 2 displays typical pharmacological sst2 features but unique dynamics of homodimerization and internalization. Endocrinology 48, 411–421.

Fan, Z.C., Sartin, J.L., Tao, Y.X., 2008. Molecular cloning and pharmacological characterization of porcine melanocortin-3 receptor. J. Endocrinol. 196, 139–148.

Feng, N., Young, S.F., Aguilera, G., Puricelli, E., Adler-Wailes, D.C., Sebring, N.G., Yanovski, J.A., 2005. Co-occurrence of two partially inactivating polymorphisms of MC3R is associated with pediatric-onset obesity. Diabetes 54, 2663–2667.

Gantz, I., Konda, Y., Tashiro, T., Shimoto, Y., Miwa, H., Munzert, G., Watson, S.J., DelValle, J., Yamada, T., 1993. Molecular cloning of a novel melanocortin receptor. J. Biol. Chem. 268, 8246–8250.

Getting, S.J., Christian, H.C., Lam, C.W., Gavins, F.N., Flower, R.J., Schioth, H.B., Perretti, M., 2003. Redundancy of a functional melanocortin 1 receptor in the anti-inflammatory actions of melanocortin peptides: studies in the recessive yellow (e/e) mouse suggest an important role for melanocortin 3 receptor. J. Immunol. 170, 3323–3330.

Getting, S.J., Gibbs, L., Clark, A.J., Flower, R.J., Perretti, M., 1999. POMC gene-derived peptides activate melanocortin type 3 receptor on murine macrophages, suppress cytokine release, and inhibit neutrophil migration in acute experimental inflammation. J. Immunol. 162, 7446–7453.

Hani, E.H., Dupont, S., Durand, E., Dina, C., Gallina, S., Gantz, I., Froguel, P., 2001. Naturally occurring mutations in the melanocortin receptor 3 gene are not associated with type 2 diabetes mellitus in French Caucasians. J. Clin. Endocrinol. Metab. 86, 2895–2898.

Herraiz, C., Garcia-Borron, J.C., Jimenez-Cervantes, C., Olivares, C., 2017. MC1R signaling. Intracellular partners and pathophysiological implications. BBA 1863, 2448–2461.

Hipkin, R.W., Deno, G., Fine, J., Sun, Y., Wilburn, B., Fan, X., Gonsiorek, W., Wiekowski, M.T., 2004. Cloning and pharmacological characterization of CXCR1 and CXCR2 from *Macaca fascicularis*. J. Pharmacol. Exp. Ther. 310, 291–300.

Humphreys, M.H., Ni, X.P., Pearce, D., 2011. Cardiovascular effects of melanocortins. Eur. J. Pharmacol. 660, 43–52.

Huszar, D., Lynch, C.A., Fairchild-Huntress, V., Dunmore, J.H., Fang, Q., Berkemeier, L.R., Gu, W., Kesterson, R.A., Boston, B.A., Cone, R.D., Smith, F.J., Campfield, L.A., Burn, P., Lee, F., 1997. Targeted disruption of the melanocortin-4 receptor results in obesity in mice. Cell 88, 131–141.

Jiang, W., Lim, H.D., Zhang, M., Desai, P., Dai, H., Colling, P.M., Leurs, R., Thurmond, R.L., 2008. Cloning and pharmacological characterization of the dog histamine H4 receptor. Eur. J. Pharmacol. 592, 26–32.

Kopin, A.S., McBride, E.W., Gordon, M.C., Quinn, S.M., Beinborn, M., 1997. Inter- and intraspecies polymorphisms in the cholecystokinin-B/gastrin receptor alter drug efficacy. Proc. Natl. Acad. Sci. U.S.A. 94, 11043–11048.

Lee, Y.S., Poh, L.K., Kek, B.L., Loke, K.Y., 2007. The role of melanocortin 3 receptor gene in childhood obesity. Diabetes 56, 2622–2630.

Lee, Y.S., Poh, L.K., Loke, K.Y., 2002. A novel melanocortin 3 receptor gene (MC3R) mutation associated with severe obesity. J. Clin. Endocrinol. Metab. 87, 1423–1426.

Li, J.T., Yang, Z., Chen, H.P., Zhu, C.H., Deng, S.P., Li, G.L., Tao, Y.X., 2016. Molecular cloning, tissue distribution, and pharmacological characterization of melanocortin-4 receptor in spotted scat, *Scatophagus argus*. Gen. Comp. Endocrinol. 230–231, 143–152.

Li, L., Yang, Z., Zhang, Y.P., He, S., Liang, X.F., Tao, Y.X., 2017. Molecular cloning, tissue distribution, and pharmacological characterization of melanocortin-4 receptor in grass carp (*Ctenopharyngodon idella*). Domest. Anim. Endocrinol. 59, 140–151.

Li, W.D., Joo, E.J., Furlong, E.B., Galvin, M., Abel, K., Bell, C.J., Price, R.A., 2000. Melanocortin 3 receptor (MC3R) gene variants in extremely obese women. Int. J. Obes. Relat. Metab. Disord. 24, 206–210.

Marks, D.L., Hruby, V., Brookhart, G., Cone, R.D., 2006. The regulation of food intake by selective stimulation of the type 3 melanocortin receptor (MC3R). Peptides 27, 259–264.

Mo, X.L., Yang, R., Tao, Y.X., 2012. Functions of transmembrane domain 3 of human melanocortin-4 receptor. J. Mol. Endocrinol. 49, 221–235.

Ndong, C., O'Donnell, D., Ahmad, S., Groblewski, T., 2011. Cloning and pharmacological characterization of the dog cannabinoid CB_2 receptor. Eur. J. Pharmacol. 669, 24–31.

Ollmann, M.M., Wilson, B.D., Yang, Y.K., Kerns, J.A., Chen, Y., Gantz, I., Barsh, G.S., 1997. Antagonism of central melanocortin receptors in vitro and in vivo by agouti-related protein. Science 278, 135–138.

Rached, M., Buronfosse, A., Begeot, M., Penhoat, A., 2004. Inactivation and intracellular retention of the human I183N mutated melanocortin 3 receptor associated with obesity. BBA 1689, 229–234.

Regard, J.B., Sato, I.T., Coughlin, S.R., 2008. Anatomical profiling of G protein-coupled receptor expression. Cell 135, 561–571.

Renquist, B.J., Murphy, J.G., Larson, E.A., Olsen, D., Klein, R.F., Ellacott, K.L., Cone, R.D., 2012. Melanocortin-3 receptor regulates the normal fasting response. Proc. Natl. Acad. Sci. U.S.A. 109, E1489–E1498.

Roselli-Rehfuss, L., Mountjoy, K.G., Robbins, L.S., Mortrud, M.T., Low, M.J., Tatro, J.B., Entwistle, M.L., Simerly, R.B., Cone, R.D., 1993. Identification of a receptor for γ melanotropin and other proopiomelanocortin peptides in the hypothalamus and limbic system. Proc. Natl. Acad. Sci. U.S.A. 90, 8856–8860.

Savastano, D.M., Tanofsky-Kraff, M., Han, J.C., Ning, C., Sorg, R.A., Roza, C.A., Wolkoff, L.E., Anandalingam, K., Jefferson-George, K.S., Figueroa, R.E., Sanford, E.L., Brady, S., Kozlosky, M., Schoeller, D.A., Yanovski, J.A., 2009. Energy intake and energy expenditure among children with polymorphisms of the melanocortin-3 receptor. Am. J. Clin. Nutr. 90, 912–920.

Schaffer, K., McBride, E.W., Beinborn, M., Kopin, A.S., 1998. Interspecies polymorphisms confer constitutive activity to the *Mastomys* cholecystokinin-B/gastrin receptor. J. Biol. Chem. 273, 28779–28784.

Tang, Y., Tan, X.M., Yue, C.W., Li, C.X., Fan, Z.X., Zhang, Y.Z., 2008. Cloning, sequence, and function analyses of giant panda (*Ailuropoda melanoleuca*) CD9 gene. Mol. Reprod. Dev. 75, 1418–1425.

Tao, Y.X., 2005. Molecular mechanisms of the neural melanocortin receptor dysfunction in severe early onset obesity. Mol. Cell. Endocrinol. 239, 1–14.

Tao, Y.X., 2007. Functional characterization of novel melanocortin-3 receptor mutations identified from obese subjects. BBA 1772, 1167–1174.

Tao, Y.X., 2010. Mutations in the melanocortin-3 receptor (MC3R) gene: impact on human obesity or adiposity. Curr. Opin. Invest. Drugs 11, 1092–1096.

Tao, Y.X., 2017. Melanocortin receptors. BBA 1863, 2411–2413.

Tao, Y.X., Huang, H., Wang, Z.Q., Yang, F., Williams, J.N., Nikiforovich, G.V., 2010. Constitutive activity of neural melanocortin receptors. Meth. Enzymol. 484, 267–279.

Tao, Y.X., Mizrachi, D., Segaloff, D.L., 2002. Chimeras of the rat and human FSH receptors (FSHRs) identify residues that permit or suppress transmembrane 6 mutation-induced constitutive activation of the FSHR via rearrangements of hydrophobic interactions between helices 6 and 7. Mol. Endocrinol. 16, 1881–1892.

Tao, Y.X., Segaloff, D.L., 2003. Functional characterization of melanocortin-4 receptor mutations associated with childhood obesity. Endocrinology 144, 4544–4551.

Tao, Y.X., Segaloff, D.L., 2004. Functional characterization of melanocortin-3 receptor variants identify a loss-of-function mutation involving an amino acid critical for G protein-coupled receptor activation. J. Clin. Endocrinol. Metab. 89, 3936–3942.

Trevaskis, J.L., Gawronska-Kozak, B., Sutton, G.M., McNeil, M., Stephens, J.M., Smith, S.R., Butler, A.A., 2007. Role of adiponectin and inflammation in insulin resistance of Mc3r and Mc4r knockout mice. Obesity (Silver Spring) 15, 2664–2672.

Wang, S.X., Fan, Z.C., Tao, Y.X., 2008. Functions of acidic transmembrane residues in human melanocortin-3 receptor binding and activation. Biochem. Pharmacol. 76, 520–530.

Wang, Z.Q., Wang, W., Shi, L., Chai, J.T., Zhang, X.J., Tao, Y.X., 2016. Molecular cloning and pharmacological characterization of giant panda (*Ailuropoda melanoleuca*) melanocortin-4 receptor. Gen. Comp. Endocrinol. 229, 32–40.

Xue, Z., Zhang, W., Wang, L., Hou, R., Zhang, M., Fei, L., Zhang, X., Huang, H., Bridgewater, L.C., Jiang, Y., Jiang, C., Zhao, L., Pang, X., Zhang, Z., 2015. The bamboo-eating giant panda harbors a carnivore-like gut microbiota, with excessive seasonal variations. MBio 6, e00022–00015.

Yang, F., Huang, H., Tao, Y.X., 2015. Biased signaling in naturally occurring mutations in human melanocortin-3 receptor gene. Int. J. Biol. Sci. 11, 423–433.

Yang, F., Tao, Y.X., 2012. Functional characterization of nine novel naturally occurring human melanocortin-3 receptor mutations. BBA 1822, 1752–1761.

Yang, Z., Tao, Y.X., 2016a. Biased signaling initiated by agouti-related peptide through human melanocortin-3 and -4 receptors. BBA 1862, 1485–1494.

Yang, Z., Tao, Y.X., 2016b. Mutations in melanocortin-3 receptor gene and human obesity. Prog. Mol. Biol. Transl. Sci. 140, 97–129.

Yi, T.L., Yang, L.K., Ruan, G.L., Yang, D.Q., Tao, Y.X., 2018. Melanocortin-4 receptor in swamp eel (*Monopterus albus*): cloning, tissue distribution, and pharmacology. Gene 678, 79–89.

Zhan, X., Li, M., Zhang, Z., Goossens, B., Chen, Y., Wang, H., Bruford, M.W., Wei, F., 2006. Molecular censusing doubles giant panda population estimate in a key nature reserve. Curr. Biol. 16, R451–452.